Spiral-Spin-Driven Ferroelectricity in a Multiferroic Delafossite $AgFeO_2$

Noriki Terada,[1,2,3] Dmitry D. Khalyavin,[2] Pascal Manuel,[2] Yoshihiro Tsujimoto,[1] Kevin Knight,[2] Paolo G. Radaelli,[3] Hiroyuki S. Suzuki,[1] and Hideaki Kitazawa[1]

[1]*National Institute for Materials Science, Sengen 1-2-1, Tsukuba, Ibaraki 305-0047, Japan*
[2]*ISIS Facility, STFC Rutherford Appleton Laboratory, Chilton, Didcot, Oxfordshire, OX11 0QX, United Kingdom*
[3]*Department of Physics, Clarendon Laboratory, University of Oxford, Parks Road, Oxford OX1 3PU, United Kingdom*

(Received 11 June 2012; published 27 August 2012)

We have performed dielectric measurements and neutron diffraction experiments on the delafossite $AgFeO_2$. A ferroelectric polarization $P \simeq 300\ \mu C/m^2$ was observed in a powder sample, below 9 K. The neutron diffraction experiment demonstrated successive magnetostructural phase transitions at $T_{N1} = 15$ K and $T_{N2} = 9$ K. The magnetic structure for 9 K $\leq T \leq$ 15 K is a spin-density wave with a temperature dependent incommensurate modulation $\boldsymbol{k} = (-1, q, \frac{1}{2})$, $q \simeq 0.384$. Below 9 K, the magnetic structure turns into elliptical cycloid with the incommensurate propagation vector $\boldsymbol{k} = (-\frac{1}{2}, q, \frac{1}{2})$, $q \simeq 0.2026$ Based on the deduced magnetic point-group symmetry $m1'$ of the low-temperature polar phase, we conclude that the ferroelectric polarization in $AgFeO_2$ is perpendicular to the monoclinic b axis and is driven by the inverse Dzyaloshinskii-Moriya effect with two orthogonal components $\boldsymbol{p}_1 \propto \boldsymbol{r}_{ij} \times (\boldsymbol{S}_i \times \boldsymbol{S}_j)$ and $\boldsymbol{p}_2 \propto \boldsymbol{S}_i \times \boldsymbol{S}_j$.

DOI: 10.1103/PhysRevLett.109.097203 PACS numbers: 75.80.+q, 75.50.Ee, 77.80.−e

In recent years, magnetoelectric multiferroic materials, which possess (anti)ferromagnetism and ferroelectricity in a single phase, have been the subject of intensive research [1,2]. In such systems, complex magnetic structures stabilized by frustrated exchange interactions between spins break inversion symmetry and induce a ferroelectric polarization. Typical examples of the materials where noncollinear spin ordering induces ferroelectric polarization are $TbMnO_3$ (Refs. [3,4]) and $CoCr_2O_4$ (Ref. [5]) with cycloidal magnetic structures. The induced ferroelectric polarization can be understood in terms of the inverse Dzyaloshinskii-Moriya (DM) effect [6] or spin current mechanism, represented by $\boldsymbol{p} \propto \boldsymbol{r}_{ij} \times (\boldsymbol{S}_i \times \boldsymbol{S}_j)$ (Ref. [7]) where $\boldsymbol{r}_{ij}$ is the vector connecting the nearest spins. On the other hand, the delafossite family, $CuFeO_2$ (Ref. [8]), $CuFe_{1-x}B_xO_2$ [B = Al and Ga (Refs. [9–11])], $CuCrO_2$ (Refs. [12,13]), and $AgCrO_2$ (Ref. [12]), shows ferroelectric polarization induced by the proper screw helical magnetic orderings $\boldsymbol{r}_{ij} || \boldsymbol{S}_i \times \boldsymbol{S}_j$ [14,15]. The magnetic field-induced ferroelectricity in $CuFeO_2$ has been explained by Arima as a combined effect of d-p hybridization and spin-orbit coupling [16].

To further understand the delafossite multiferroic materials, we have studied the magnetodielectric properties of $AgFeO_2$. While $CuFeO_2$ has been extensively investigated as a frustrated magnet [17–19] and a multiferroic material [8–11,14], $AgFeO_2$ has not been studied due to lack of a high-quality sample. Nevertheless, Tsujimoto *et al.*. have recently succeeded in the synthesis under high pressure [20]. Although neutron diffraction measurements were reported recently, no details of the magnetic structure were presented [21].

The crystal structure of $AgFeO_2$, which is shown in Fig. 1(a), belongs to rhombohedral space group $R\bar{3}m$, and has the lattice constants, $a = b = 3.0391(1)$ Å and $c = 18.5899(9)$ Å at room temperature. For later convenience, the monoclinic unit cell stable at low temperature is also depicted in Fig. 1(a). The triangular layers formed by magnetic Fe^{3+} ions (surrounded with distorted oxygen octahedra) are stacked in a rhombohedral sequence and in-between nonmagnetic Ag^{1+} cations are incorporated separating the magnetic layers.

Vasiliev *et al.* [21] and Tsujimoto *et al.* [20] have reported the temperature dependence of the magnetic susceptibility revealing successive phase transitions at ~15 K (T_{N1}) and ~9 K (T_{N2}) [Fig. 2(a)]. In the present study, in order to investigate the microscopic spin structures and dielectric properties of $AgFeO_2$, we have performed neutron diffraction experiments and dielectric measurements using high-quality polycrystalline samples.

Powder specimens of delafossite $AgFeO_2$ were prepared under high pressure as described in Ref. [20]. The electric polarization and dielectric constant were measured using 1.25 mm thickness hardened pellet of polycrystalline $AgFeO_2$ sample covered with an area 19.6 mm^2 of silver paste. The electric polarization was determined by conventional pyroelectric current measurements using a Keithley 6517E electrometer. For the dielectric measurements, we used an Agilent E4980A LCR meter. The neutron powder diffraction measurements were carried out on WISH [22] and HRPD [23] time-of-flight diffractometers at ISIS Facility, United Kingdom. Crystal and magnetic structure refinements were performed using the FULLPROF program [24]. We first refined the data measured on HRPD to get precisely the crystal structure parameters; subsequently,

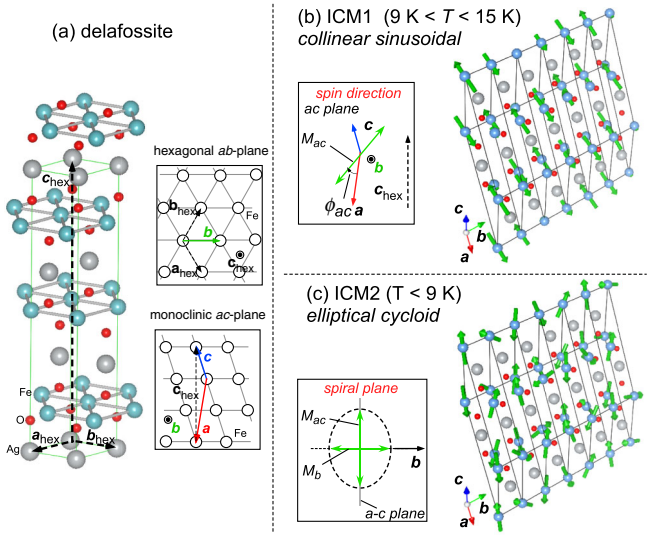

FIG. 1 (color online). (a) The delafossite crystal structure of $AgFeO_2$ with both hexagonal and monoclinic bases. (b) Collinear sinusoidally modulated magnetic structure in ICM1 phase for 9 K $\leq T \leq$ 15 K. (c) Cycloidal structure with elliptical modulation in ICM2 phase for $T \leq 9$ K. The insets are schematic pictures to explain the relationship between these spin directions and crystal axis.

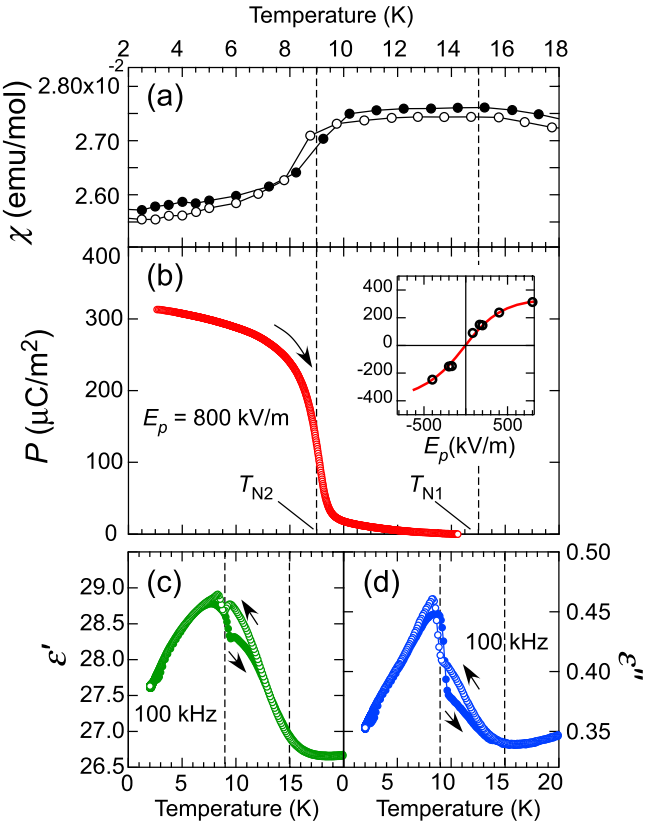

FIG. 2 (color online). (a) Magnetic susceptibility (data taken from Ref. [20]), (b) electric polarization, (c) real and (d) imaginary parts of the dielectric constant of a powder sample of $AgFeO_2$ as a function of temperature. The inset in (b) is the poling electric field dependence of the polarization.

the data measured on WISH were refined to determine the magnetic ordering while the structural parameters were fixed to the values obtained from the HRPD data.

As shown in Fig. 2(b), the electric polarization P appears only below the lower phase transition temperature $T_{N2} = 9$ K. The absolute value of P is 313 $\mu C/m^2$ in the poling electric field, $E_p = 800$ kV/m, which is close to the saturation value [see the inset of Fig. 2(b)]. Since a powder sample was used in the measurements, P is a half of the intrinsic value for a single crystal, namely $P_{\text{intrinsic}} \simeq 600$ $\mu C/m^2$, which is comparable to that of the typical multiferroics [1,8]. The temperature dependence of the real part of the dielectric constant, shown in Fig. 2(c), demonstrates a clear anomaly at T_{N2}, in agreement with the pyroelectric measurements. The imaginary part of the dielectric constant [Fig. 2(d)] corresponding to the energy dissipation, increases with decreasing temperature below $T_{N1} = 15$ K, then exhibits a peak at $T_{N2} = 9$ K, and eventually decreases gradually below 9 K. The relatively large energy dissipation might be caused by the finite correlation lengths in both magnetic phases, which is discussed below.

Based on the HRPD and WISH backscattering data revealing a clear splitting of some nuclear peaks below T_{N1}, a symmetry lowering from the rhombohedral $R\bar{3}m$ down to monoclinic $C2/m$ can be concluded. In addition, a set of magnetic Bragg reflections appears below this temperature (Fig. 3), which can be indexed by the incommensurate propagation vector $\boldsymbol{k} = (-1, q, \frac{1}{2})$ with $q \simeq 0.384$, referring to the monoclinic cell shown in Fig. 1(a). The wave number q depends on temperature and cooling or heating process, as shown in the inset of Figs. 3 and 4(b). Note that the $\boldsymbol{k}$ in the monoclinic setting corresponds to the $(q', q', \frac{3}{2})$ with $q' \simeq 0.192$ in the hexagonal cell, which is almost identical to that found in the partially disordered state of $CuFeO_2$ [25]. The width of the magnetic peaks in the ICM1 phase is slightly wider than the instrumental resolution width depicted by the horizontal bar in the inset of Fig. 3. As shown in Fig. 4(c), the correlation length is about 200–600 Å (65–200 sites), and significantly depends on temperature.

Below $T_{N2} = 9$ K (ICM2 phase), a set of new magnetic reflections indexed by the propagation vector $\boldsymbol{k} = (-\frac{1}{2}, q, \frac{1}{2})$ with $q \simeq 0.206$ appears [Figs. 3 and 4(a)]. At $T = 9$ K, the reflections from both ICM1 and ICM2 phases coexist upon heating or cooling processes, indicating a first order phase transition. The propagation vector in the ICM2 phase also slightly depends on temperature, and does not lock in any commensurate value even at the lowest measured temperature 5 K [Fig. 4(b)]. As shown in Fig. 4(c), the correlation length remains finite ~500 Å (~ 165 sites) at the lowest temperature, as evidenced by the peak width, which is wider than the resolution limit (inset of Fig. 3).

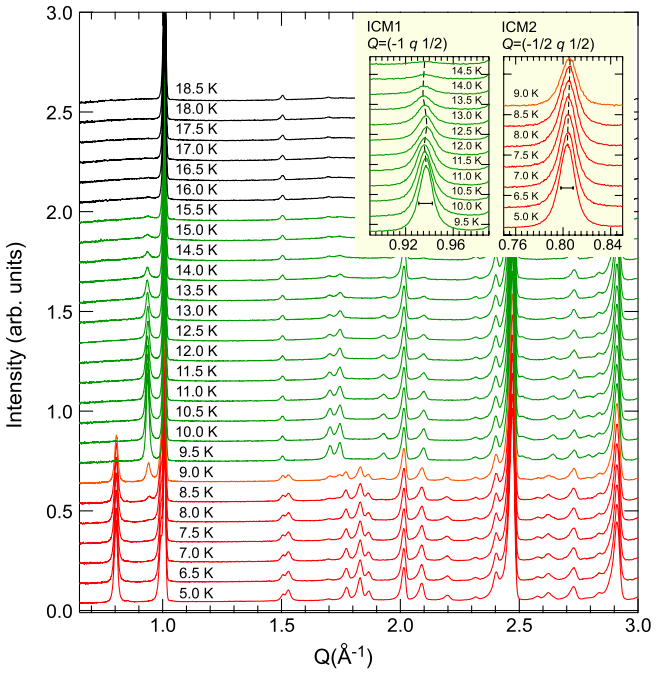

FIG. 3 (color online). Temperature dependence of the neutron powder diffraction profiles of $AgFeO_2$. The inset shows the expansions of profiles in low-Q regions in ICM1 and ICM2 phase. The data were taken on heating process on WISH. The horizontal bars denote the experimental resolution at each position.

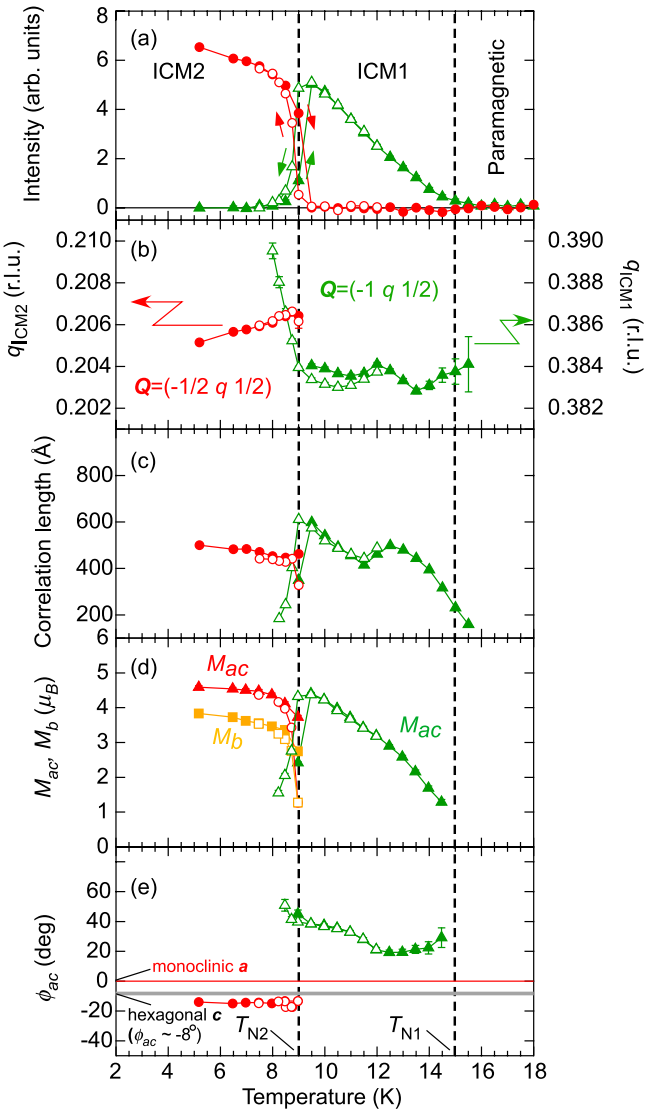

FIG. 4 (color online). Temperature dependence of (a) the integrated intensity of the magnetic Bragg reflections, (b) the propagation wave numbers, (c) the correlation lengths for $(-1, q, \frac{1}{2})$ and $(-\frac{1}{2}, q, \frac{1}{2})$. Temperature dependence of (d) the magnetic momentum components, M_{ac} and M_b, and (e) the angle between the spin direction projected into ac plane and the crystal a axis ϕ_{ac}. Closed and open symbols denote data measured with heating and cooling processes, respectively.

For the ICM1 phase with $\boldsymbol{k} = (-1, q, \frac{1}{2})$, we successfully refined the diffraction data using the monoclinic $C2/m$ space group for the nuclear scattering and the collinear sinusoidally modulated spin structure [Fig. 1(b)] for the magnetic scattering. The quality of the refinement is demonstrated in Fig. 5(a). The symmetry of the magnetic phase preserves the structural point group and contains time inversion as a separate element due to the incommensurate nature of the spin ordering. Thus, the magnetic point group in the ICM1 phases is the centro-symmetric $2/m1'$ in agreement with the lack of the polarization in the dielectric measurements (Fig. 2). The tilt angle of the spin-density plane from the a axis toward the c axis ϕ_{ac} depends significantly on temperature, $20^\circ \leq \phi_{ac} \leq 50^\circ$, as illustrated in Fig. 4(e). These spin directions are considerably different from $\phi'_{ac} \simeq 10^\circ$ in $CuFeO_2$ [26], implying that A-site cation (Cu^{1+} or Ag^{1+}) plays an important role in determining the magnetic anisotropy in these systems, as suggested in a recent x-ray absorption spectroscopy study [27].

For the ICM2 phase with $\boldsymbol{k} = (-\frac{1}{2}, q, \frac{1}{2})$, the magnetic contribution to the diffraction data [Fig. 5(b)] can be refined in the model with the noncollinear cycloidal spin arrangement [Fig. 1(c)]. The cycloid is elliptically modulated with the spin components in the ac plane and along the b axis being $M_{ac} = 4.56(4)\mu_B$ and $M_b = 3.81(5)\mu_B$, respectively, at $T = 5$ K. The angle between the elliptical axis (perpendicular to b) and a axis in the ac plane is $\phi_{ac} = -14.6(8)^\circ$, which is very close to the c direction of the hexagonal cell [see thick solid line in Fig. 4(e)]. The cycloidal magnetic ordering breaks the inversion symmetry but preserves the mirror plane perpendicular to the b axis. Therefore, the magnetic point group in the ICM2 phase is the polar $m1'$, which is consistent with the polarization measurements (Fig. 2). The obtained results clearly demonstrate the difference in the magnetic ground stats of $AgFeO_2$ and $CuFeO_2$. The latter compound exhibits commensurate $\boldsymbol{k} = (-1, 1/2, 1/2)$ magnetic ordering with collinear $\uparrow\uparrow\downarrow\downarrow$ spin arrangement along hexagonal [110]

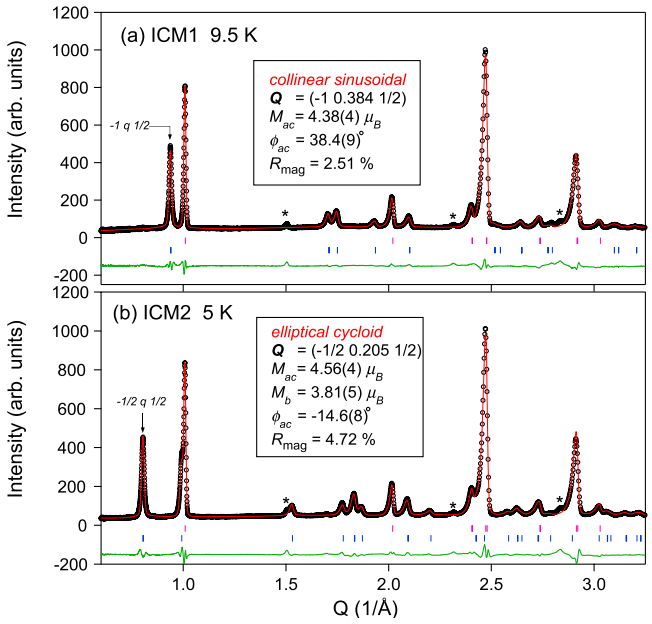

FIG. 5 (color online). Typical results of the magnetic structural refinement for the experimental data measured with WISH at (a) 9.5 and (b) 5 K. The vertical bars indicate magnetic and nuclear (upper row) Bragg peaks, and the stars indicate the reflection from a small amount impurity contained in the sample. The refined parameters and reliability factors are written in these insets.

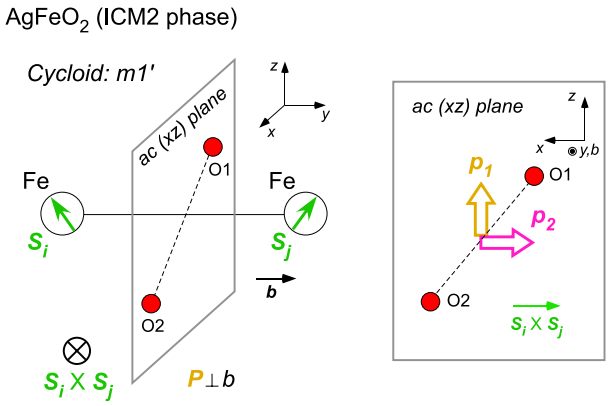

FIG. 6 (color online). (left) Illustration of two spins in the cycloidal structure with two oxygen atoms in $AgFeO_2$. (right) Directions of two possible electric dipole moments in the ac plane $\boldsymbol{p}_1 \propto \boldsymbol{r}_{ij} \times (\boldsymbol{S}_i \times \boldsymbol{S}_j)$ and $\boldsymbol{p}_2 \propto \boldsymbol{S}_i \times \boldsymbol{S}_j$. x, y, and z is (anti)parallel to $\boldsymbol{S}_i \times \boldsymbol{S}_j$, parallel to b, and perpendicular to them, respectively.

direction [28]. Thus, the nonmagnetic A-site cation plays a crucial role in the delafossite ferrites not only for the magnetic anisotropy but also for the exchange interactions.

Let us discuss the direction of $\boldsymbol{P}$ in the ICM2 phase based on the deduced magnetic point-group symmetry and recent theoretical works. The $m1'$ symmetry restricts the polarization direction to be parallel to the mirror plane ($\boldsymbol{P} \perp b$). Considering the well-known theory of inverse DM effect [6] or spin current mechanism [7], represented by $\boldsymbol{p} \propto \boldsymbol{r}_{ij} \times (\boldsymbol{S}_i \times \boldsymbol{S}_j) (\equiv \boldsymbol{p}_1)$, $\boldsymbol{P}$ is expected to be perpendicular to both $\boldsymbol{r}_{ij}$ and $\boldsymbol{S}_i \times \boldsymbol{S}_j$, i.e., along the z axis in Fig. 6 (this direction is very close to the hexagonal c axis). However, an additional contribution to the polarization $\boldsymbol{p}_2 \propto \boldsymbol{S}_i \times \boldsymbol{S}_j$ is also expected by symmetry since the mixed product $\boldsymbol{p}_2 \cdot \boldsymbol{S}_i \times \boldsymbol{S}_j$ is invariant under all symmetry operations of $C2/m1'$. Kaplan and Mahanti have shown that this additional term $\boldsymbol{p}_2$ contributes to macroscopic polarization in both cycloidal and proper screw helical cases unless mirror plane containing $\boldsymbol{r}_{ij}$ or twofold rotation axis perpendicular to $\boldsymbol{r}_{ij}$ exist [29]. Since $\boldsymbol{p}_2$ is perpendicular to $\boldsymbol{p}_1$ (see Fig. 6), the direction of the macroscopic polarization in $AgFeO_2$ should not be restricted by the well-known formula [2,6,7]. Although the mechanism causing the appearance of $\boldsymbol{P}$ is the inverse DM effect, its direction is given by the sum of the two components $\boldsymbol{p}_1 + \boldsymbol{p}_2$. It should be pointed out here that the $\boldsymbol{p}_2$ component parallel to $\boldsymbol{S}_i \times \boldsymbol{S}_j$ is also applicable for other delafossite compounds ABO_2 (A = Cu, Ag, B = Fe, Cr) where the spin ordering breaks the threefold and inversion symmetry [8–13]. Finally, we should mention that the calculations based on the spin-dependent d-p hybridization mechanism [16] also yield $\boldsymbol{P} \perp b$.

In conclusion, a ferroelectric polarization $P \simeq 300\ \mu\mathrm{C/m^2}$ was observed in a polycrystalline sample of delafossite $AgFeO_2$ below $T_{N2} = 9$ K. The appearance of the polarization is related to cycloidal spin ordering with the incommensurate propagation vector $\boldsymbol{k} = (-\frac{1}{2}, q, \frac{1}{2})$, with $q \simeq 0.206$, resulting in the polar magnetic point-group $m1'$. Above T_{N2}, the spins are ordered into spin-density wave with the modulation vector $\boldsymbol{k} = (-1, q, \frac{1}{2})$, with $q \simeq 0.384$ and nonpolar point-group symmetry $2/m1'$. The polar magnetic ground state of $AgFeO_2$ is drastically different from the nonpolar commensurate state of $CuFeO_2$, testifying the crucial role of the nonmagnetic A-site cation. The induced macroscopic polarization can be understood in terms of the inverse Dzyaloshinskii-Moriya effect with two orthogonal components $\boldsymbol{p}_1 \propto \boldsymbol{r}_{ij} \times (\boldsymbol{S}_i \times \boldsymbol{S}_j)$ and $\boldsymbol{p}_2 \propto \boldsymbol{S}_i \times \boldsymbol{S}_j$.

The authors wish to thank T. Nakajima for useful discussion and T. Yamaguchi for technical support in dielectric measurements. The images shown in Fig. 1 were depicted using the software VESTA [30] developed by K. Monma. This work is supported by an international collaboration research program, "Young Researcher Overseas Visits Program for Vitalizing Brain Circulation" of JSPS. N. T. is supported by the JSPS Postdoctoral Fellowships for Research Abroad.

[1] T. Kimura, T. Goto, H. Shintani, K. Ishizaka, T. Arima, and Y. Tokura, Nature (London) **426**, 55 (2003).
[2] S.-W. Cheong and M. Mostovoy, Nature Mater. **6**, 13 (2007).

[3] M. Kenzelmann, A. B. Harris, S. Jonas, C. Broholm, J. Schefer, S. B. Kim, C. L. Zhang, S.-W. Cheong, O. P. Vajk, and J. W. Lynn, Phys. Rev. Lett. **95**, 087206 (2005).
[4] T. Arima, A. Tokunaga, T. Goto, H. Kimura, Y. Noda, and Y. Tokura, Phys. Rev. Lett. **96**, 097202 (2006).
[5] Y. Yamasaki, S. Miyasaka, Y. Kaneko, J.-P. He, T. Arima, and Y. Tokura, Phys. Rev. Lett. **96**, 207204 (2006).
[6] I. A. Sergienko and E. Dagotto, Phys. Rev. B **73**, 094434 (2006).
[7] H. Katsura, N. Nagaosa, and A. V. Balatsky, Phys. Rev. Lett. **95**, 057205 (2005).
[8] T. Kimura, J. C. Lashley, and A. P. Ramirez, Phys. Rev. B **73**, 220401(R) (2006).
[9] S. Kanetsuki, S. Mitsuda, T. Nakajima, D. Anazawa, H. A. Katori, and K. Prokes, J. Phys. Condens. Matter **19**, 145244 (2007).
[10] S. Seki, Y. Yamasaki, Y. Shiomi, S. Iguchi, Y. Onose, and Y. Tokura, Phys. Rev. B **75**, 100403(R) (2007).
[11] N. Terada, T. Nakajima, S. Mitsuda, H. Kitazawa, K. Kaneko, and N. Metoki, Phys. Rev. B **78**, 014101 (2008).
[12] S. Seki, Y. Onose, and Y. Tokura, Phys. Rev. Lett. **101**, 067204 (2008).
[13] K. Kimura, H. Nakamura, K. Ohgushi, and T. Kimura, Phys. Rev. B **78**, 140401(R) (2008).
[14] T. Nakajima, S. Mitsuda, K. Takahashi, M. Yamano, K. Masuda, H. Yamazaki, K. Prokes, K. Kiefer, S. Gerischer, N. Terada, H. Kitazawa, M. Matsuda, K. Kakurai, H. Kimura, Y. Noda, M. Soda, M. Matsuura, and K. Hirota, Phys. Rev. B **79**, 214423 (2009).
[15] M. Soda, K. Kimura, T. Kimura, M. Matsuura, and K. Hirota, J. Phys. Soc. Jpn. **78**, 124703 (2009).
[16] T. Arima, J. Phys. Soc. Jpn. **76**, 073702 (2007).
[17] M. Mekata, N. Yaguchi, T. Takagi, T. Sugino, S. Mitsuda, H. Yoshizawa, N. Hosoito, and T. Shinjo, J. Phys. Soc. Jpn. **62**, 4474 (1993).
[18] S. Mitsuda, M. Mase, K. Prokes, H. Kitazawa, and H. A. Katori, J. Phys. Soc. Jpn. **69**, 3513 (2000).
[19] O. A. Petrenko, G. Balakrishnan, M. R. Lees, D. M. Paul, and A. Hoser, Phys. Rev. B **62**, 8983 (2000).
[20] Y. Tsujimoto *et al.* (unpublished).
[21] A. Vasiliev, O. Volkova, I. Presniakov, A. Baranov, G. Demazeau, J.-M. Broto, M. Millot, N. Leps, R. Klingeler, B. Büchner, M. B. Stone, and A. Zheludev, J. Phys. Condens. Matter **22**, 016007 (2010).
[22] L. C. Chapon, P. Manuel, P. G. Radaelli, C. Benson, L. Perrott, S. Ansell, N. J. Rhodes, D. Raspino, D. Duxbury, E. Spill, and J. Norris, Neutron News **22**, 22 (2011).
[23] R. M. Ibberson, W. I. F. David, and K. S. Knight, Rutherford Appleton Laboratory, Chilton, Didcot, England Report No. RAL-92-031, 1992.
[24] J. Rodriguez-Carvajal, Physica (Amsterdam) **192B**, 55 (1993).
[25] S. Mitsuda, N. Kasahara, T. Uno, and M. Mase, J. Phys. Soc. Jpn. **67**, 4026 (1998).
[26] N. Terada, T. Kawasaki, S. Mitsuda, H. Kimura, and Y. Noda, J. Phys. Soc. Jpn. **74**, 1561 (2005).
[27] M. Malvestuto, F. Bondino, E. Magnano, T. T. A. Lummen, P. H. M. van Loosdrecht, and F. Parmigiani, Phys. Rev. B **83**, 134422 (2011).
[28] F. Ye, Y. Ren, Q. Huang, J. A. Fernandez-Baca, P. Dai, J. W. Lynn, and T. Kimura, Phys. Rev. B **73**, 220404(R) (2006).
[29] T. A. Kaplan and S. D. Mahanti, Phys. Rev. B **83**, 174432 (2011).
[30] K. Momma and F. Izumi, J. Appl. Crystallogr. **41**, 653 (2008).